ACS APPLIED MATERIALS & INTERFACES

Research Article

www.acsami.org

Regenerative Astaxanthin Extraction from a Single Microalgal (*Haematococcus pluvialis*) Cell Using a Gold Nano-Scalpel

Ramasamy Praveenkumar,[†,‡,@] Raekeun Gwak,[§,@] Mijeong Kang,[§] Tae Soup Shim,[⊥] Soojeong Cho,[∥] Jiye Lee,[†] You-Kwan Oh,[†] Kyubock Lee,*[,†] and Bongsoo Kim*[,§]

[†]Biomass and Waste Energy Laboratory, Korea Institute of Energy Research, Daejeon 34129, Korea

[‡]Department of Chemistry and Bioengineering, Tampere University of Technology, Tampere 33720, Finland

[§]Department of Chemistry and [∥]Department of Chemical and Biomolecular Engineering, KAIST, Daejeon 34141, Korea

[⊥]Department Chemical Engineering, Ajou University, Suwon 16499, Korea

Supporting Information

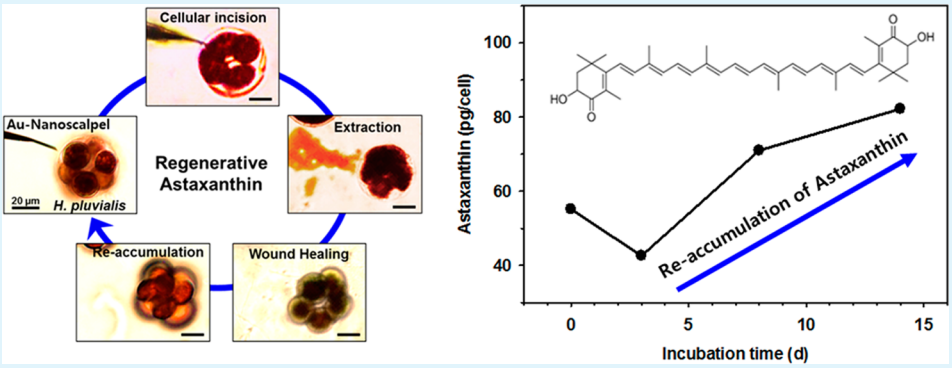

ABSTRACT: Milking of microalgae, the process of reusing the biomass for continuous production of target compounds, can strikingly overcome the time and cost constraints associated with biorefinery. This process can significantly improve production efficiency of highly valuable chemicals, for example, astaxanthin (AXT) from *Haematococcus pluvialis*. Detailed understanding of the biological process of cell survival and AXT reaccumulation after extraction would be of great help for successful milking. Here we report extraction of AXT from a single cell of *H. pluvialis* through incision of the cell wall by a gold nanoscalpel (Au-NS), which allows single-cell analysis of wound healing and reaccumulation of AXT. Interestingly, upon the Au-NS incision, the cell could reaccumulate AXT at a rate two times faster than the control cells. Efficient extraction as well as minimal cellular damage, keeping cells alive, could be achieved with the optimized shape and dimensions of Au-NS: a well-defined sharp tip, thickness under 300 nm, and 1−3 μm of width. The demonstration of regenerative extraction of AXT at a single cell level hints toward the potential of a milking process for continuous recovery of target compounds from microalgae while keeping the cells alive.

KEYWORDS: *regenerative extraction, wound-healing, mechanotransduction, astaxanthin, nanoscalpel, microalgae*

INTRODUCTION

Microalgae are attractive feedstocks for high-value compounds such as carotenoids and docosahexaenoic acid (DHA) as well as biofuels.[1−4] Microalgal biorefinery, however, involves multiple steps such as cultivation, harvesting, and product extraction, which accumulates in time and cost constraints for commercial scale production. Recently, it has been suggested that milking of microalgae can significantly reduce the time and cost of this process.[5−7] The idea is to reuse the biomass for the continuous production of the compound just like milking cows.

Unlike the conventional biorefinery, requiring a time-consuming cultivation step and an intensively energy-consuming harvesting step, the milking process does not require reculturing of cells from the exponential stage of the cultivation process nor harvesting,[5−7] and the target compounds are continuously extracted from cells which keep accumulating the compounds. Although some experiments suggested possibilities of the milking processes,[5,7] in order to fully exploit the merits of the milking processes, we would need more detailed and an in-depth study on the biological process of living microalgae that can directly observe product reaccumulation, which could be done by a carefully controlled single-cell level study.

The upsurge in development of nanoscale fabrication provides new ways to manipulate biological processes at the single-cell level.[8−11] Particularly, one-dimensional nanostructures such as nanowires can be employed as efficient membrane-penetrating delivery systems that provide both

Received: August 18, 2015
Accepted: September 23, 2015
Published: September 23, 2015

DOI: 10.1021/acsami.5b07651
ACS Appl. Mater. Interfaces 2015, 7, 22702−22708

biocompatibility and high spatial resolution with their extremely small diameter and high aspect ratio. While successful applications of nanoneedle technologies to animal cell studies have been demonstrated,[12,13] the rigid cell walls of microalgae and difficulty of fixing a single cell make application of the nanoneedle to microalgal study quite challenging.[14] For successful cell-penetration of microalgae, optimum properties in size, mechanical strength, and sharpness of the nanoneedle need to be assured.

The goal of this study is to investigate the possibility to regeneratively extract astaxanthin (AXT), a ketocartenoid and a high-value chemical with wide nutraceutical applications,[15−20] from *Haematococcus pluvialis*. We developed a single crystalline gold nanoscalpel (Au-NS) to incise a *H. pluvialis* cell and extract AXT then directly observed reaccumulation of AXT at a single cell level, demonstrating a successful milking process. Successful incision of the rigid cell wall of *H. pluvialis* while maintaining cellular integrity was achieved through the unique properties of a Au-NS: a well-defined sharp tip with atomically smooth surface, uniform width along the whole length, and high mechanical strength. Furthermore, this article reports on the incision-induced mechanotransduction accelerating AXT accumulation, which reflects the potential of regenerative extraction process in microalgal biorefinery. Establishing a successful milking process for such a microalgae could be a significant breakthrough in biorefinery.

RESULTS AND DISCUSSION

Figure 1 shows the process of regenerative extraction of AXT from *H. pluvialis*, by incising the cell wall using a Au-NS,

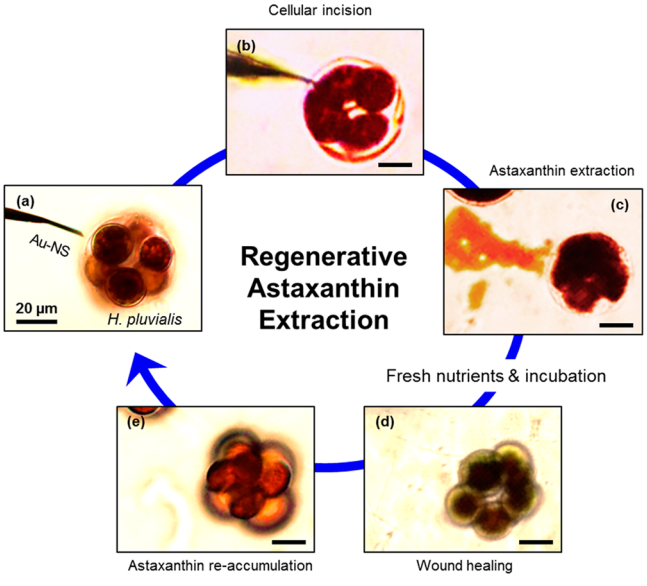

Figure 1. (a−e) Illustration of the process of the regenerative astaxanthin extraction from a single *H. pluvialis* with a Au-NS manipulator.

followed by cellular wound healing and reaccumulation of AXT. Figure 1 (panels a−c) shows that red-colored AXT was extracted from a dividing *H. pluvialis* by Au-NS manipulation. After incubation with fresh nutrients, the incised cell was healed and completed the division while maintaining its cellular metabolism (Figure 1d). Upon further incubation, the divided cells reaccumulated astaxanthin, from which the extraction process can be repeated (Figure 1e). We followed the time course changes in a single incised cell while keeping the neighbor cells as references (Figure 2). The changes in the red

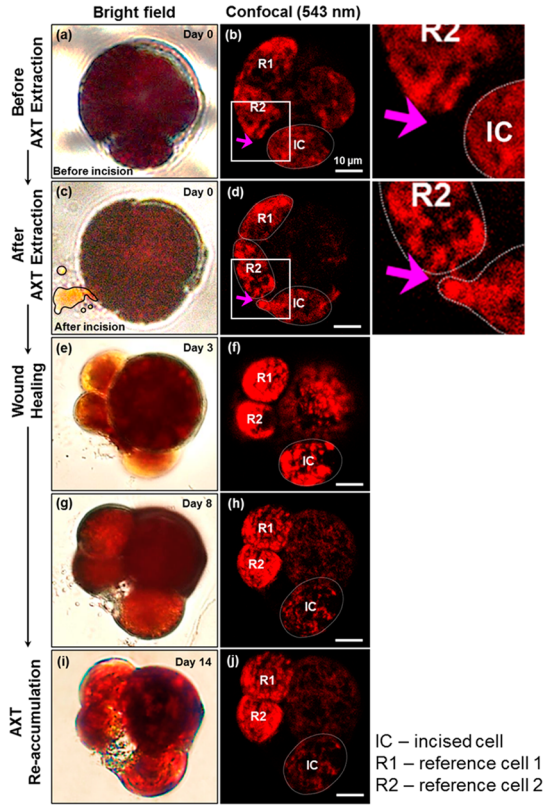

Figure 2. CLSM imaging of cell survival and chlorophyll changes in a dividing cyst of *H. pluvialis* incised using a Au-NS (a and b) and (c and d) bright field and CLSM images of a dividing cyst before and after Au-NS based incision, respectively. Black color guide map (in c) and an arrow (in d) indicates the AXT extraction out of the cell and the direction of Au-NS incision, respectively. (b1 and d1) Zoomed images of the area shown under rectangle mark in images (b and d, respectively), (e and f), (g and h), (i and j) bright field and CLSM images of a dividing cyst at the 3rd, 8th, and 14th day after Au-NS-based incision. IC, R1, and R2 represent the incised cell and reference cell nos. 1 and 2 among bright field and confocal fluorescence images.

pigmentation (AXT) and the chlorophyll autofluorescence were followed under bright field and also under 543 nm laser through confocal microscopy, respectively. In the series of the milking process, Figure 2 (panels c and d, e and f, and g−j) corresponds to AXT extraction, wound healing, and reaccumulation of AXT, respectively. As the first step of a milking process, Figure 2 (panels a−d) shows successful incision of a single cell by a Au-NS (c.a. three μm width) that resulted in extraction of AXT from the cell. In fact, the extract includes chlorophyll from the disturbed thylakoids in addition to AXT, which is accumulated lipid droplets.[23] Chlorophyll, having autofluorescence, leaves a mark of Au-NS taken out of the cell as indicated by an arrow representing the AXT extraction out of the cell in Figure 2 (panels d and d1). In the next step, addition of nutrients stopped bleeding of pigments and increased chlorophyll content in the incised cell to a level similar to the reference cells R1 and R2, which is essential to maintaining cellular metabolism (day 3; Figure 2, panels e and f). The inhibition of pigment release and the increase in chlorophyll autofluorescence indicates that the cell had successfully undergone wound healing, the only means by which an incised

DOI: 10.1021/acsami.5b07651
ACS Appl. Mater. Interfaces 2015, 7, 22702−22708

cell could return to its regular metabolic activities. Upon prolonged incubation, AXT gradually reaccumulated in the cell (~ day 14) as observed under bright field microscopy (Figure 2, panels g and i).

Superb physical and chemical properties of Au makes Au nanostructures quite popular for live cell micromanipulation.[13,21,22,24] However, considering the cells are only 10−20 μm in size, an incision in the range of a few micrometers could be fatal for metabolic activity of the cell. Here, successful regenerative AXT extraction was presumably achieved by developing Au-NS in such a way as to minimize physical damage to the cells. Au-NSs were synthesized by a chemical vapor transport method, where the vaporized gold atoms were carried to sapphire substrates and then aggregated on the substrates to form half-octahedral seeds (Figure S4). The seed has well-defined facets and atomically smooth Au (111) surfaces. The seed develops into a scalpel-like structure as time passes while maintaining its well-defined crystal geometry. As shown in Figures 3 and S5, the width and thickness of the

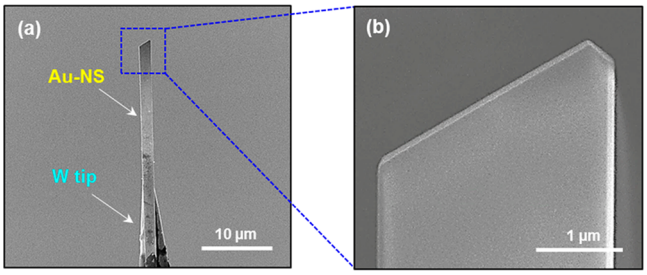

Figure 3. (a and b) SEM images of a Au-NS at different magnifications.

Au-NS are maintained along its whole length unlike the nanoneedles fabricated by chemical etching and having a tapered tip shape. Here, the tips and edges of Au-NS were established sharp, and all the facets of Au-NSs are ultraflat allowing Au-NS to craft a smooth incision in a cell. Taken together, morphological strength of Au-NSs makes them suitable for cell membrane incision to minimize cellular damage. Furthermore, the width of a nanoscalpel was controlled from 300 nm to 5 μm by varying the reaction time while maintaining its thickness of 100−300 nm (Figure S3).

The width-to-thickness ratio of a Au-NS grown from seed crystals can be controlled by varying the ratio of the supply rate of atoms which leads direct collision of Au vapor to those by surface diffusion. Thus, size of Au-NS can be finely tuned for incising cell wall by adjusting the deposition flux.

The Au-NSs of different widths (c.a. 300 nm, 800 nm, 3 μm, and 5 μm) were tested for the microextraction and regeneration of AXT in a *H. pluvialis* cell (Figures S3a-b, 1a, and S3c). Successful incisions were made with Au-NSs of width 800 nm and 3 μm, following which the cells, upon incubation, underwent wound healing and remained alive. Wound healing in this study represents the process of recovery of the incised cells to their normal metabolic activity as observed under a microscope with their chlorophyll accumulation (Figure 2, panels e and f). While the extraction of pigments from the cell was very weak with 800 nm wide Au-NS due to the smaller incision made in the cell wall, the cell did not survive after incision with a 5 μm wide Au-NS.

Moreover, owing to their larger size, the 5 μm wide Au-NS damaged also the neighboring cells and resulted in death (Figure S6). This implies the significance of a critical incision size for selective incision and regenerative AXT extraction. While a few studies reported on wound healing of macroalgae or chemical defense mechanisms upon random disruption of phytoplanktons through stimulations such as osmotic stress,[25−28] this is the first demonstration of wound healing of unicellular microalgae by physically generating the wound with well-defined sizes and the following direct microscopical observation.

With the Au-NS (3 μm of width) manipulation system, a specific single cell could be selected and incised to release the AXT among many divided daughter cells with high spatial resolution (Figure 4). The controlled germination of a matured

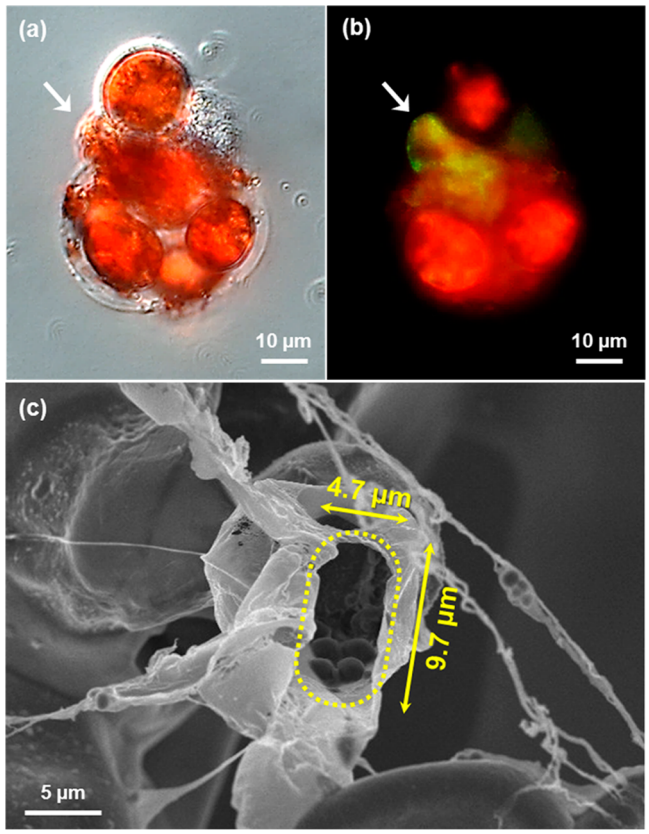

Figure 4. Microscopical images of cells incised with a 3 μm width Au-NS. (a) Bright field image of an incised cell with astaxanthin out of the cell. (b) Fluorescence image of the incised cell stained with SYTOX green. The cell with incision takes up the stain and appears green under fluorescence imaging. (c) SEM image of the incised cell. The explanations for the bigger size of the wound are provided under Figure S8.

red cyst results in formation of daughter cells (Figure S7). The germination and the selective incision of a single cell among multiple daughter cells are quite important in this work, since we can monitor the time-dependent change of the incised cell in comparison with the neighboring control cells under exactly the same culture condition and environment. The bright field image shows that the red pigment, AXT, is extracted and spread out around the incised cell indicated by the white arrow (Figure 4a). Since it is hardly discernible whether a single cell was incised or not by the observation under the bright field, cells

DOI: 10.1021/acsami.5b07651
ACS Appl. Mater. Interfaces 2015, 7, 22702−22708

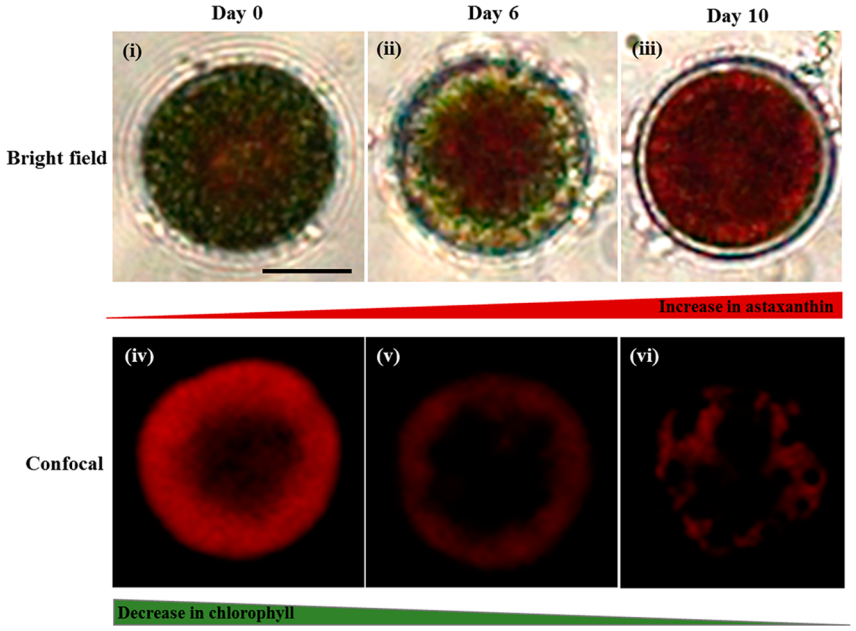

Figure 5. Relationship between astaxanthin accumulation and chlorophyll degradation. (a, b, and c) Bright field optical micrographs of *H. pluvialis* at different stages of growth, showing an increase in accumulation of astaxanthin in the cell. (d, e, and f) CLSM micrographs of *H. pluvialis* at different stages of growth showing a decrease in chlorophyll autofluorescence.

were stained with SYTOX green which is taken up only through the damaged cell wall. Figure 4b shows that the single cell which appears green under fluorescence microscopy is selectively incised. Figures 4c and S8b show scanning electron microscopic (SEM) images of a single cell incised using a Au-NS after freeze-drying. The incision of *H. pluvialis* cell by Au-NS left a slit-like hole in their cell wall. Although the size of the hole was enlarged during freeze-drying (Figure S8, panels c and d) and the dimensions of the hole do not represent the actual incision size, the slitlike hole reflects the cross-sectional shape of Au-NS (Figure 4c).

We employed confocal laser scanning microscope (CLSM) along with digital image analysis to establish an indirect but more reasonable method to quantify the AXT concentrations at a single-cell level. We took advantage of the characteristic of *H. pluvialis*, which contains chlorophyll and AXT as major pigments, the proportions of which are a trade-off depending on the cell stage.[23] The accumulation of the AXT pigment in the *H. pluvialis* cell (red color under bright field; Figure 5 (panels a, b, and c) was inversely proportional to the chlorophyll content inside the cell (red color under 543 nm laser; Figure 5 (panels d, e, and f). With the presence of the porphyrin ring, chlorophyll emits red color autofluorescence on laser excitation at 543 nm, whereas the AXT pigment does not have autofluorescence and displays a red color under bright-field microscopy. We obtained a linear relationship between the cellular chlorophyll concentration and the relative chlorophyll autofluorescence values (Figure 6a). Further, an exponential inverse relationship between the concentrations of cellular AXT from bulk samples with their relative chlorophyll autofluorescence values was established through the calibration curve (Figure 6a). The relationship achieved out of calibration of AXT concentration against the chlorophyll autofluorescence value allows a direct microscopic measurement of AXT content of a single *H. pluvialis* cell (Figure 6b). After microextraction and addition of nutrients, the concentration of AXT decreased by day 3 as we expected, since an active cellular metabolism resulting in degradation of the secondary carotenoid also accumulates primary carotenoids and photosynthetic pigments such as chlorophylls for photosynthetic cell growth.[29−31] However, upon further incubation, the concentration of AXT gradually increased and, to our surprise, the final AXT content of the extracted cell was quantified as 82 pg/cell, twice as high as the reference cells that were undisturbed (Figure 6b). Such an increase in the concentration of the secondary carotenoid could be expected from the nature of *H. pluvialis*, tending to accumulate high levels of AXT out of cellular defense mechanism in response to stress.[29] The high stress experienced by the microextracted cell could have stimulated such an increase in final AXT concentrations. It could be inferred from the present result that under controlled conditions, after extraction of AXT from the cell, the wound healing is followed by a reaccumulation of AXT with higher vigor than the normal cells. The present results clearly display the possibilities and potential cues toward the concept of milking that could aid development of alternative strategies for successful continuous extraction systems for high value compounds while keeping the cells alive. For practical-scale milking, cell germination could be potentially applied to weaken the cell wall,[4] and treating the cells with biocompatible and target-specific solvents in a two-phase continuous flow reactor[5] could be an economically feasible process.

CONCLUSION

We report a regenerative AXT extraction from a single microalgal cell using a single crystalline Au-NS. Successful incision of the rigid cell wall of *H. pluvialis* was achieved while minimizing cellular damage, which allowed the direct observation of AXT extraction and reaccumulation in a single cell. Importantly, our results, showing the increase of AXT accumulation induced by nanoincision, propose a new type of mechanotransduction accelerating the induction of the target compounds in microalgae. It is expected that the Au-NS nanoincision system not only provides insights toward a

DOI: 10.1021/acsami.5b07651
ACS Appl. Mater. Interfaces 2015, 7, 22702−22708

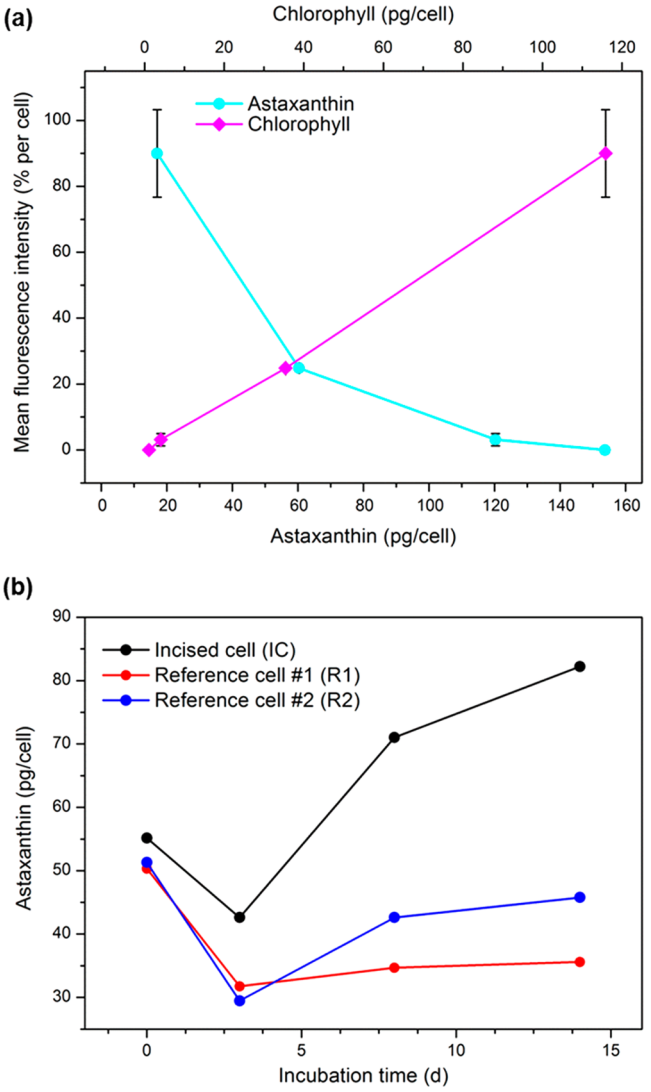

Figure 6. (a) Calibration curve for chlorophyll and astaxanthin concentration based on the autofluorescence pixel count from 40 cells at different stages of growth against their actual concentrations from bulk samples (pg/cell), respectively. (b) Comparison of relative astaxanthin content among the incised and two reference cells (nos. 1 and 2) at 0, 3, 8, and 14 d following incision. The relative astaxanthin content was calculated based on the autofluorescence pixel intensity values against the calibration plot. (Note: CLSM images were obtained under identical acquisition parameters allowing this comparison to be made.)

promising strategy of microalgal milking process but also could be widely used for the study of cell biology such as gene delivery by single cell manipulation, especially with rigid cell walls such as microalgae.

EXPERIMENTAL DETAILS

***Haematococcus pluvialis* Cultivation and Controlled Germination.** *Haematococcus pluvialis* (strain NIES-144, University of Tokyo, Japan) was grown in the NIES-C medium. A single colony grown on an agar plate was transferred to a 250 mL Erlenmeyer flask (working volume, 100 mL). The flasks were incubated in a shaking incubator at 25 °C and 150 rpm. The light was supplied continuously for 14 days with 40 μmol/m^{2}s by four white fluorescent lamps.[4] Astaxanthin (AXT) induction was carried out by transferring the cells to the NIES-N medium (see Supporting Information M1 for medium composition).

The mature red cysts (30 to 50 μm of dia) were gravitationally settled in agarose microwells (30 μm of depth and 50 μm of dia) inside a Gene Frame chamber (see Supporting Information M1 and Figure S1 for details regarding patterning of microwell). Further the cysts were allowed to germinate under controlled conditions by gently spreading 25 μL of 0.5 × NIES-C medium over the agarose microwell and allowed to dry for 5 min inside a sterile laminar hood. The chamber was then covered with a detachable coverslip and incubated in a growth chamber (Lab Companion, Jeio Tech) at 25 °C for 2 days. The samples were illuminated at 25 μmol/m^{2}s by four white fluorescent lamps continuously. Germination of red cyst cells into the agarose microwells were verified using a Zeiss Imager A2 microscope (Zeiss, Germany) equipped with DIC optics.

Gold Nanoscalpel (Au-NS) Synthesis. Single-crystalline Au-NSs were synthesized on a c-cut sapphire substrate in a horizontal quartz tube furnace system using a previously described vapor transport method (Figure S2).[21] Au lump in an alumina boat was placed at the middle of the heating zone and sapphire substrates were placed at a few centimeters downstream from the Au lump. The Au lump was heated to 1130 °C, while 100 sccm flow of Ar gas and 3−5 Torr of chamber pressure were maintained. The vaporized Au atoms were carried to the substrate via Ar flow and subsequently formed Au seeds then vertically grew into nanobelts. Structural features of Au-NSs can be controlled by adjusting synthetic conditions such as substrate position, heating temperature, chamber pressure, and reaction time. Especially, the width can be controlled by adjusting the reaction time while maintaining similar thickness.

For convenient manipulation, a single Au-NS was fixed on a macroscopic tungsten tip. The tungsten tip touched one of the vertically grown Au-NSs and detached it from the substrate by van der Waals force. For solid fixation of the Au-NS on the tungsten tip, the interfacing region between them was covered by UV-hardening polymer and exposed to a UV lamp for 2 h.

Single-Cell Incision. The system for fixing *H. pluvialis* and manipulating a single cell using a Au-NS is composed of microalgal cells, *H. pluvialis*, in an agarose microwell cultivation chamber, Au-NS manipulator, and an optical microscope (Figure S2a). The *H. pluvialis* cells fixed inside the agarose microwells (Figure S2b), following germination, were incised using a Au-NS by pushing the cell against the walls of the microwells at an angle approximately between 5 and 15° to the plane of agarose. The Au-NS was mounted on a three-dimensional piezoelectric stage, through which their movement could be controlled with high spatial resolution (<200 nm).[13,21,22] Au-NS of various widths (c.a. 300 nm, 800 nm, 3 μm, and 5 μm) were tested to incise the divided cells of *H. pluvialis* (Figure S3, panels a and b, 1a and S3d). The process of microextraction through the Au-NS was controlled and monitored under a bright field microscope (Zeiss, Germany).

Microscopic Monitoring of Incised Cell. Following cellular incision and release of AXT, the Gene Frame chamber was flooded with ∼20 μL of 0.5 × NIES-C medium and allowed to dry for 2 min inside a sterile laminar hood and incubated in a growth chamber (Lab Companion, Jeio Tech) at 25 °C and were illuminated at 25 μmol/m^{2}s by four white fluorescent lamps continuously. The changes in the manipulated cells were monitored at regular intervals using a Zeiss Imager A2 fluorescence microscope (Zeiss, Germany) equipped with DIC optics.

Selective incision of single cells using a Au-NS was confirmed through SYTOX green (Life Technologies) staining. Following incision using a Au-NS (∼3 μm width), the cell was treated with 5 μL of 5 mM SYTOX Green for 2 min and rinsed twice with sterile distilled water under microscope (Zeiss, Germany). The chlorophyll autofluorescence and SYTOX green signals were detected through a long pass filter set 09 (excitation filter: 450−490 nm band-pass; BS FT: 510 nm; EM LP: 515 nm; Zeiss, Germany). The images were captured through an AxioCam HRc CCD camera with AxioVision software (Zeiss, Germany).

The reaccumulation of AXT in the incised *H. pluvialis* cell was characterized using a confocal laser scanning microscope (CLSM; LSM 5 PASCAL, Zeiss, Germany). Signals from chlorophyll

DOI: 10.1021/acsami.5b07651
ACS Appl. Mater. Interfaces 2015, 7, 22702−22708

autofluorescence were detected by excitation with helium−neon laser at 543 nm, and the emissions over 560 nm were captured by using the long path filter. All the CLSM images were obtained under identical acquisition parameters, allowing the comparison to be made for relative quantification through image analysis.

■ ASSOCIATED CONTENT

Supporting Information

The Supporting Information is available free of charge on the ACS Publications website at DOI: 10.1021/acsami.5b07651.

Detailed methodologies on culturing *H. pluvialis*, patterning of agarose microwells and analytical methodologies, schematic illustrations of the experimental system, microscopic images of Au-NSs incising single cell, scheme of reactor to synthesis Au-NSs, SEM image of Au-NS, and micrographs of controlled germination (PDF)

■ AUTHOR INFORMATION

Corresponding Authors

*E-mail: kyubock.lee@kier.re.kr.

*E-mail: bongsoo@kaist.ac.kr.

Author Contributions

[@]R.P. and R.G. contributed equally.

Notes

The authors declare no competing financial interest.

■ ACKNOWLEDGMENTS

This study was supported by the R&D Program of the KIER (B5-2450). Further support was received from the Advanced Biomass R&D Center (ABC) of the Global Frontier Project funded by the Ministry of Science, ICT and Future Planning (ABC- 2012M3A6A205388), and by the KETEP and MKE of Korea as a part of the "Process demonstration for bioconversion of CO_2 to high-valued biomaterials using microalgae" (20152010201900) project of the "Energy Efficiency and Resources R&D project". This work was also supported by the Public Welfare & Safety research program (NRF-2012M3A2A1051682, NRF-2012M3A2A1051686) through the NRF of Korea funded by MSIP. We thank Alan West for the English editing of the manuscript.

■ REFERENCES

(1) Georgianna, D. R.; Mayfield, S. P. Exploiting Diversity and Synthetic Biology for the Production of Algal Biofuels. *Nature* **2012**, *488*, 329−335.

(2) Wijffels, R. H.; Barbosa, M. J. An Outlook on Microalgal Biofuels. *Science* **2010**, *329*, 796−799.

(3) Foley, P. M.; Beach, E. S.; Zimmerman, J. B. Algae as a Source of Renewable Chemicals: Opportunities and Challenges. *Green Chem.* **2011**, *13*, 1399−1405.

(4) Praveenkumar, R.; Lee, K.; Lee, J.; Oh, Y.-K. Breaking Dormancy: An Energy-Efficient Means of Recovering Astaxanthin from Microalgae. *Green Chem.* **2015**, *17*, 1226−1234.

(5) Hejazi, M.; Andrysiewicz, E.; Tramper, J.; Wijffels, R. Effect of Mixing Rate on β-Carotene Production and Extraction by *Dunaliella Salina* in Two-Phase Bioreactors. *Biotechnol. Bioeng.* **2003**, *84*, 591−596.

(6) Hejazi, M. A.; Wijffels, R. H. Milking of Microalgae. *Trends Biotechnol.* **2004**, *22*, 189−194.

(7) Zhang, F.; Cheng, L.-H.; Xu, X.-H.; Zhang, L.; Chen, H.-L. Screening of Biocompatible Organic Solvents for Enhancement of Lipid Milking from *Nannochloropsis* sp. *Process Biochem.* **2011**, *46*, 1934−1941.

(8) Chen, X.; Kis, A.; Zettl, A.; Bertozzi, C. R. A Cell Nanoinjector Based on Carbon Nanotubes. *Proc. Natl. Acad. Sci. U. S. A.* **2007**, *104*, 8218−8222.

(9) Obataya, I.; Nakamura, C.; Han, S.; Nakamura, N.; Miyake, J. Nanoscale Operation of a Living Cell Using an Atomic Force Microscope with a Nanoneedle. *Nano Lett.* **2005**, *5*, 27−30.

(10) Yan, R.; Park, J.-H.; Choi, Y.; Heo, C.-J.; Yang, S.-M.; Lee, L. P.; Yang, P. Nanowire-Based Single-Cell Endoscopy. *Nat. Nanotechnol.* **2011**, *7*, 191−196.

(11) Yum, K.; Na, S.; Xiang, Y.; Wang, N.; Yu, M.-F. Mechanochemical Delivery and Dynamic Tracking of Fluorescent Quantum Dots in the Cytoplasm and Nucleus of Living Cells. *Nano Lett.* **2009**, *9*, 2193−2198.

(12) Jeffries, G. D.; Edgar, J. S.; Zhao, Y.; Shelby, J. P.; Fong, C.; Chiu, D. T. Using Polarization-Shaped Optical Vortex Traps for Single-Cell Nanosurgery. *Nano Lett.* **2007**, *7*, 415−420.

(13) Yoo, S. M.; Kang, M.; Kang, T.; Kim, D. M.; Lee, S. Y.; Kim, B. Electrotriggered, Spatioselective, Quantitative Gene Delivery into a Single Cell Nucleus by Au Nanowire Nanoinjector. *Nano Lett.* **2013**, *13*, 2431−2435.

(14) Hawes, C.; Osterrieder, A.; Sparkes, I. A.; Ketelaar, T. Optical Tweezers for the Micromanipulation of Plant Cytoplasm and Organelles. *Curr. Opin. Plant Biol.* **2010**, *13*, 731−735.

(15) Chew, B.; Park, J.; Wong, M.; Wong, T. A Comparison of the Anticancer Activities of Dietary Beta-Carotene, Canthaxanthin and Astaxanthin in Mice in vivo. *Anticancer Res.* **1999**, *19*, 1849−1853.

(16) Han, D.; Li, Y.; Hu, Q. Astaxanthin in Microalgae: Pathways, Functions and Biotechnological Implications. *Algae* **2013**, *28*, 131−147.

(17) Guerin, M.; Huntley, M. E.; Olaizola, M. *Haematococcus* Astaxanthin: Applications for Human Health and Nutrition. *Trends Biotechnol.* **2003**, *21*, 210−216.

(18) Lorenz, R. T.; Cysewski, G. R. Commercial Potential for *Haematococcus* Microalgae as a Natural Source of Astaxanthin. *Trends Biotechnol.* **2000**, *18*, 160−167.

(19) Mayne, S. T. Beta-Carotene, Carotenoids, and Disease Prevention in Humans. *FASEB J.* **1996**, *10*, 690−701.

(20) Wang, X.; Willén, R.; Wadström, T. Astaxanthin-Rich Algal Meal and Vitamin C Inhibit *Helicobacter Pylori* Infection in BALB/cA Mice. *Antimicrob. Agents Chemother.* **2000**, *44*, 2452−2457.

(21) Yoo, Y.; Seo, K.; Han, S.; Varadwaj, K. S.; Kim, H. Y.; Ryu, J. H.; Lee, H. M.; Ahn, J. P.; Ihee, H.; Kim, B. Steering Epitaxial Alignment of Au, Pd, and AuPd Nanowire Arrays by Atom Flux Change. *Nano Lett.* **2010**, *10*, 432−438.

(22) Kang, T.; Yoo, S. M.; Yoon, I.; Lee, S. Y.; Kim, B. Patterned Multiplex Pathogen DNA Detection by Au Particle-on-Wire SERS Sensor. *Nano Lett.* **2010**, *10*, 1189−1193.

(23) Yoon, I.; Kang, T.; Choi, W.; Kim, J.; Yoo, Y.; Joo, S.-W.; Park, Q.-H.; Ihee, H.; Kim, B. Single Nanowire on a Film as an Efficient SERS-Active Platform. *J. Am. Chem. Soc.* **2009**, *131*, 758−762.

(24) Wayama, M.; Ota, S.; Matsuura, H.; Nango, N.; Hirata, A.; Kawano, S. Three-Dimensional Ultrastructural Study of Oil and Astaxanthin Accumulation during Encystment in the Green Alga *Haematococcus pluvialis*. *PLoS One* **2013**, *8*, e53618.

(25) Gu, Y.; Sun, W.; Wang, G.; Zimmermann, M. T.; Jernigan, R. L.; Fang, N. Revealing Rotational Modes of Functionalized Gold Nanorods on Live Cell Membranes. *Small* **2013**, *9*, 785−792.

(26) Pohnert, G. Wound-Activated Chemical Defense in Unicellular Planktonic Algae. *Angew. Chem., Int. Ed.* **2000**, *39*, 4352−4354.

(27) Pohnert, G. Phospholipase A2 Activity Triggers the Wound-Activated Chemical Defense in the Diatom *Thalassiosira Rotula*. *Plant Physiol.* **2002**, *129*, 103−111.

(28) La Claire, J. W. Cytomorphological Aspects of Wound Healing in Selected Siphonocladales (Chlorophyceae). *J. Phycol.* **1982**, *18*, 379−384.

(29) Kim, G. H.; Lee, I. K.; Fritz, L. The Wound-Healing Responses of *Antithamnion Nipponicum* and *Griffithsia Pacifica* (Ceramiales, Rhodophyta) Monitored by Lectins. *Phycol. Res.* **1995**, *43*, 161−166.

DOI: 10.1021/acsami.5b07651
ACS Appl. Mater. Interfaces 2015, 7, 22702−22708

(30) Boussiba, S. Carotenogenesis in the Green Alga *Haematococcus Pluvialis*: Cellular Physiology and Stress Response. *Physiol. Plant.* **2000**, *108*, 111−117.
(31) Damiani, M. C.; Leonardi, P. I.; Pieroni, O. I.; Cáceres, E. J. Ultrastructure of the Cyst Wall of *Haematococcus Pluvialis* (Chlorophyceae): Wall Development and Behaviour during Cyst Germination. *Phycologia* **2006**, *45*, 616−623.

DOI: 10.1021/acsami.5b07651
ACS Appl. Mater. Interfaces 2015, 7, 22702−22708